

## Tale of two- $U(1)$ axion models

Dong Hu<sup>1,\*</sup> Hao-Ran Jiang<sup>1,†</sup> Hao-Lin Li<sup>2,‡</sup> Ming-Lei Xiao<sup>2,§</sup> and Jiang-Hao Yu<sup>2,3,4,5,||</sup>

<sup>1</sup>*Department of Physics and State Key Laboratory of Nuclear Physics and Technology, Peking University, Beijing 100871, China*

<sup>2</sup>*CAS Key Laboratory of Theoretical Physics, Institute of Theoretical Physics, Chinese Academy of Sciences, Beijing 100190, China*

<sup>3</sup>*School of Physical Sciences, University of Chinese Academy of Sciences, Beijing 100049, China*

<sup>4</sup>*School of Fundamental Physics and Mathematical Sciences, Hangzhou Institute for Advanced Study, University of Chinese Academy of Sciences, Hangzhou 310024, China*

<sup>5</sup>*International Center for Theoretical Physics Asia-Pacific, Beijing/Hangzhou 100190, China*



(Received 25 January 2021; accepted 26 April 2021; published 24 May 2021)

$U(1)$  global symmetry to solve the strong  $CP$  problem could be a remnant of multi- $U(1)$  symmetries from QCD and hidden strong dynamics. Both Peccei-Quinn  $U(1)$  and dynamical  $U(1)$  are described uniformly, based on which we classify various mixed two- $U(1)$  models to solve both strong  $CP$  and quality problems. We propose a moose diagram method with different fermion assignments to directly read relations between  $CP$  phases, which illustrate how the strong  $CP$  problem is solved in terms of cancellation between  $CP$  phases. In two-axion models, we find that the lightest axion is still the same as a QCD axion in the infrared region, while a one-axion model with  $Z_2$  symmetry enhances the axion mass spectrum. Our discussions can be extended to multi-axion cases.

DOI: [10.1103/PhysRevD.103.095025](https://doi.org/10.1103/PhysRevD.103.095025)

### I. INTRODUCTION

In the 1970s, 't Hooft proposed that QCD has a nontrivial vacuum structure and solved the  $U(1)_A$  problem [1,2]. The nontrivial vacuum structure suggests that there is an additional topological term which violates  $CP$  symmetry in the QCD Lagrangian. The  $CP$ -violating term brings a free parameter denoted as  $\theta$ . Because of the axial anomaly, a chiral rotation of quarks changes  $\theta$  and the argument involving Yukawa couplings of quarks, while the sum of them is invariant. Thus, the observable strong  $CP$  phase in the Standard Model (SM) is

$$\bar{\theta} = \theta + \arg \det(Y_u Y_d), \quad (1)$$

where  $u, d$  represent up and down type quarks, respectively. A measurement of the neutron electric dipole moment (EDM) suggests that  $|\bar{\theta}| < 10^{-10}$  [3]. How to understand

the extreme smallness of  $\bar{\theta}$  is the well-known strong  $CP$  problem.

There are several ways to solve the strong  $CP$  problem. One solution is the Nelson-Barr mechanism [4,5], which assumes  $CP$  to be conserved at the high energy scale. That is, the  $CP$ -violating phases of the Cabibbo-Kobayashi-Maskawa (CKM) matrix and  $\bar{\theta}$  are both zero at the high energy scale, while at the low energy scale the  $CP$ -violating phase  $\delta$  of the CKM matrix is reproduced and  $\bar{\theta}$  is still fixed at zero. An alternative approach is to utilize the chiral rotation of the fermions to absorb  $\bar{\theta}$  when a massless quark or an additional global chiral  $U(1)$  symmetry exists. However, a solution with a massless quark was disfavored by the results of lattice QCD with  $m_u = 2.2^{+0.5}_{-0.4}$  MeV [6]. The additional global chiral  $U(1)$  solution was first proposed by Peccei and Quinn [7,8]. Later, Weinberg [9] and Wilczek [10] predicted that a pseudoscalar such as the Goldstone boson called an axion would result from the spontaneous breaking of this additional  $U(1)_{PQ}$  symmetry. Although the original Weinberg-Wilczek axion model has been ruled out by experiments [11], derived models still survive. The Kim-Shifman-Vainshtein-Zakharov (KSVZ) [12,13] and Dine-Fischler-Srednicki-Zhitnisky (DFSZ) [14,15] models are the most typical ones.

Although the KSVZ and DFSZ models survive from experimental constraints, there exists an additional theoretical issue, the quality problem. Constraints from astrophysics give the lower bound of the decay constant of the

\*hudong16@pku.edu.cn

†h.r.jiang@pku.edu.cn

‡lihaolin@itp.ac.cn

§mingleix@itp.ac.cn

||jhyu@itp.ac.cn

Published by the American Physical Society under the terms of the [Creative Commons Attribution 4.0 International license](https://creativecommons.org/licenses/by/4.0/). Further distribution of this work must maintain attribution to the author(s) and the published article's title, journal citation, and DOI. Funded by SCOAP<sup>3</sup>.

axion as  $f_a \gtrsim 10^8$  GeV [16]. There is a general consensus that gravitational effects generate operators suppressed by the Planck scale  $M_{\text{Pl}}$  which explicitly break global symmetries. As with the axion model, the explicit breaking effect is estimated by the operators [17,18]

$$V(\phi) = g \frac{|\phi|^{2m} \phi^n}{M_{\text{Pl}}^{2m+n-4}} + \text{H.c.} \quad (2)$$

Although these operators are suppressed by the Planck scale, the smallness of the strong  $CP$  phase and the high scale of  $\langle \phi \rangle \sim f_a$  cause non-negligible effects from the lower-dimensional operators. Consequentially, the minimum of the scalar potential is shifted and the  $CP$  phase  $\bar{\theta}$  reappears. To solve this problem, one can impose a discrete symmetry  $Z_N$  with a large  $N$  on  $\phi$  so that operators with a dimension less than  $N$  are forbidden. For  $f_a = 10^{12}$  GeV, a scale at which the axion can serve as dark matter, operators with a dimension  $2m + n < 14$  are forbidden [19]. Another idea is to reduce the vacuum expectation value (VEV)  $\langle \phi \rangle$  while preserving a large  $f_a$ . Implementation is accomplished in multiple axion models using the alignment mechanism [20–22] or the clockwork mechanism [23]. On the other hand, a very heavy axion with  $m_a \gtrsim O(100)$  MeV evades the astrophysical constraints [24], and thus a small  $f_a$  is allowed to relax the quality problem. Furthermore, in some composite axion models, gauge invariance forbids operators of high dimensions by arranging fermions suitably [25]. In this paper we focus on the simplest multiple axion model, the two-axion model.

On the other hand, an additional non-Abelian gauge group is often introduced in various new physics, such as hidden valley [26], vectorlike confinement [27], and twin Higgs [28]. These extensions of the SM are usually motivated by the hierarchy problem or dark matter. Furthermore, the  $U(1)$  global symmetry to solve the strong  $CP$  problem could be a remnant of multi- $U(1)$  symmetry from the hidden strong dynamics. We call this kind of non-Abelian gauge group “hidden QCD” in this paper.

As in SM QCD, hidden QCD may contain the  $CP$  violation source from the  $\theta' G' \tilde{G}'$  term and the relevant fermion Yukawa couplings, although it may or may not influence the observed neutron EDM. Besides the QCD theta term, there are three types of effective operators contributing directly to the neutron EDM, including the quark EDM, the quark chromo EDM, and the three-gluon Weinberg operator [29,30]:

$$\begin{aligned} O_d &= -\frac{i}{2} d \bar{q} \sigma^{\mu\nu} \gamma_5 q F_{\mu\nu}, \\ O_{\tilde{d}} &= -\frac{i}{2} \tilde{d} \bar{q} \sigma^{\mu\nu} t^a \gamma_5 q G_{\mu\nu}^a, \\ O_w &= \frac{1}{3} w f^{abc} G_{\mu\nu}^a \tilde{G}_{\nu\beta}^b G_{\beta\mu}^c, \end{aligned} \quad (3)$$

where  $d$  denotes EDM,  $\tilde{d}$  denotes chromo EDM,  $t^a$  is the generator of the QCD group, and  $f^{abc}$  denotes the QCD structure constant. The  $\theta' G' \tilde{G}'$  term in hidden QCD is not directly related to these operators. However, two typical scenarios will result in the sensitivity of the neutron EDM to the  $CP$  violation in the hidden sector:

- (a) Two strong  $CP$  angels can be associated with each other by introducing a pseudoscalar. The interaction between the pseudoscalar and gauged fermions and the chiral rotation of the pseudoscalar are

$$\begin{aligned} \mathcal{L} &\sim y_q e^{ina/f_a} q \bar{q} + y_Q e^{ima/f_a} Q \bar{Q} + \text{H.c.}, \\ a/f_a &\rightarrow a/f_a + \alpha, \quad \theta \rightarrow \theta - n\alpha, \quad \theta' \rightarrow \theta' - m\alpha, \end{aligned} \quad (4)$$

where  $q$  and  $Q$  notate fermions charged under QCD and hidden QCD, respectively.  $a$  is the pseudoscalar.  $n$  and  $m$  are constants.

- (b) Fermions charged under both QCD and hidden QCD can link these two  $CP$  phases. The chiral rotation of these fermions can change both phases such that

$$\begin{aligned} \psi_L(N_c, N_h) &\rightarrow \psi_L(N_c, N_h) e^{i\beta}, \quad \theta \rightarrow \theta - N_h \beta, \\ \theta' &\rightarrow \theta' - N_c \beta, \end{aligned} \quad (5)$$

where  $N_c$  and  $N_h$  are representations of fermions in QCD and hidden QCD, respectively.

Under such circumstances, both  $\theta$  and  $\theta'$  have observable impacts on the strong  $CP$  problem, as either the Peccei-Quinn symmetry or the chiral rotation of massless fermion can transfer the  $\theta(\theta')$  term into  $\theta'(\theta)$ . Consequently, the physical  $CP$ -violating angle in QCD related to the neutron EDM is the linear combination of the two theta angles. Therefore, these two angles must be small simultaneously to explain the strong  $CP$  problem. Either two global chiral  $U(1)$  symmetries are needed or there is one chiral  $U(1)$  symmetry with a  $Z_2$  among the two sectors. In this work, we focus on the first scenario, while the latter is discussed in Refs. [24,31–35].

Chiral  $U(1)$  symmetries are classified into one of two groups depending upon whether the corresponding axion is elementary or composite. We refer to the one generating an elementary axion as the  $U(1)_{PQ}$  arising from the phase of a complex scalar, and the one generating a composite axion (also called a dynamical axion [36]) as the  $U(1)_A$  arising when massless fermions of the hidden QCD condense at the high energy scale. In the infrared region, the two scenarios share a similar nature and the pseudoscalars are the Goldstones of these chiral  $U(1)$  symmetries that are named axions. Instanton effects explicitly break these symmetries and determine the properties of the axion, such as mass and axion-photon coupling. Therefore, new instanton effects of the hidden QCD could enlarge axion

mass in some models with  $Z_2$  symmetry [24,31,37], and they could also enhance axion-photon coupling in [38]. Moreover, an additional strong dynamics also provides solutions to the quality and domain wall problems [39].

With hidden QCD introduced, we find new mixed  $U(1)$  solutions which contain two sorts of chiral  $U(1)$  symmetries. In these cases, spontaneous symmetry breaking of  $U(1)_{PQ}$  could be triggered by the dynamical symmetry breaking in the hidden sector, in addition to the conventional Ginzburg-Landau potential method. The cancellation of  $CP$  phases is always viable, except in alignment situations. The cancellation of  $CP$  phases in the QCD and the hidden QCD sector is shown in Sec. III. The lightest axion in these models is similar to the QCD axion. Some phenomena of these models are discussed in Sec. IV.

In addition to the new mixed  $U(1)$  solution mentioned above, we also propose a ‘‘mooselike’’ diagram method to visualize the cumbersome relations among gauge groups, new fields and  $CP$  phases in multi-axion models, from which the  $U(1)$  charges for the fields and the potentials of the relevant axions and  $CP$  phases can be easily read. Moreover, the diagram method helps one to construct models containing more  $U(1)$  and gauge groups.

This paper is organized as follows. In Sec. II, we discuss two typical patterns to realize chiral  $U(1)$ . Next, in Sec. III, we give solutions of the strong  $CP$  problem and propose a diagram method to present these solutions. In Sec. IV, we study the axion mass, axion-photon coupling, and axion decay constant of one-axion solutions and two typical mixed two-axion solutions. We summarize the results in Sec. V.

## II. PECCI-QUINN OR DYNAMICAL SOLUTION

A large class of models solve the strong  $CP$  problem by adding additional global  $U(1)$  symmetries. There are mainly two kinds of  $U(1)$ 's: the one in the Pecci-Quinn mechanism [7,8], denoted as  $U(1)_{PQ}$ , is associated with a elementary scalar  $\phi$ , while the other is the axial  $U(1)_A$  of some massless fermions charged under gauge groups, which induces the dynamical solution [36].

Although  $U(1)_{PQ}$  and  $U(1)_A$  symmetries have different origins in the ultraviolet region, they solve the strong  $CP$  problem with the same philosophy: to make the  $CP$  phase dynamically canceled by introducing a  $U(1)$  pseudo Goldstone boson (PGB) with an anomaly-induced potential. In both scenarios, there are fermions that are axially charged under the global  $U(1)$ ,

$$f_L \rightarrow e^{i\alpha} f_L, \quad f_R \rightarrow e^{-i\alpha} f_R. \quad (6)$$

However, the  $U(1)$  is broken in different ways: in the Pecci-Quinn mechanism, it is broken by the scalar potential  $V(\phi)$  and the PGB turns out to be  $a \sim \arg \phi$ , the axion; in the dynamical solution, it is broken by condensation of the

TABLE I. Fermion charge and representation.

	$SU(3)_c$	$SU(3)_h$	$U(1)_{PQ}$
$\psi$	3	3	0
$\chi$	1	3	0
$Q$	3	1	$m$
$Q'$	1	3	$n$

fermions, and the PGB is a composite of the fermion, also known as the dynamical axion. The common infrared behavior is that both PGBs correspond to some axial currents whose conservation is broken only by anomaly. This inspires a general description of these models, as presented in the following.

In this section, we propose a mooselike diagram method to uniformly illustrate the structures of the models solving the strong  $CP$  problem. The notation of all possible additional fermions introduced are listed in Table I. As an example, we show the structure of the aligned axion model [20] in Fig. 1(a) and that of the dynamical axion model [36] in Fig. 1(b). In Fig. 1(a), we list all the axions, with each representing a global  $U(1)$ , normalized as their proper contributions to the  $CP$  phase. Dashed lines link the axions to the fermions, and the numbers along them indicate the corresponding  $U(1)$  charges of the fermions. The solid lines with tags show the nontrivial representations of the fermions under the linked gauge groups in Fig. 1(b), like the color  $SU(3)_c$  and the hidden  $SU(3)_h$ . Circles on the vertices represent massive fermions; crosses on the vertices represent massless fermions.

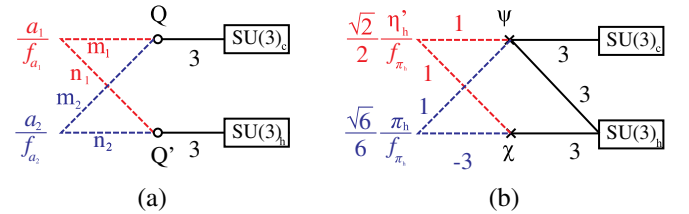


FIG. 1. (a) Solid line between  $Q$  and  $SU(3)_c$  showing that  $Q$  is under representation 3 of QCD and the solid line between  $Q'$  and  $SU(3)_h$  showing that  $Q'$  is under representation 3 of hidden QCD. The red dashed line between  $a_1$  and  $Q(Q')$  shows that the charge of  $Q(Q')$  under  $U(1)_{PQ}$  is  $m_1$  ( $n_1$ ). Similarly, the blue dashed line shows that the charge of  $Q(Q')$  under  $U(1)_{PQ'}$  is  $m_2$  ( $n_2$ ).  $1/f_{a_1}$  and  $1/f_{a_2}$  are scale factors for two  $U(1)$ 's. (b) Solid lines showing that  $\psi$  is under representation 3 for both QCD and hidden QCD, and that  $\chi$  is a singlet for QCD but under representation 3 for hidden QCD. The red dashed lines show that the ratio of  $\psi$  and  $\chi$  in the  $\eta'_h$  current is 1:1, which is similar to the  $U(1)$  charge in (a) in the infrared region. The only difference is one more normalization factor  $\sqrt{2}/2$  in front of the scale factor  $1/f_{\pi_h}$ . Similarly, blue lines show that the ratio of  $\psi$  and  $\chi$  in the  $\pi_h$  current is 1:–3. The normalization factor is  $\sqrt{6}/6$  and the scale factor is  $1/f_{\pi_h}$ .

The alignment axion model has been widely discussed in the literature [20,21,40].  $SU(3)_h$  is introduced with a new free parameter of  $CP$  violation  $\theta'$ . As shown in Fig. 1(a), massive fermions  $Q(3, 1)$  and  $Q'(1, 3)$  are charged under both  $U(1)_{PQ}$  symmetry and  $U(1)_{PQ'}$  symmetry. When  $U(1)_{PQ}$  and  $U(1)_{PQ'}$  are broken, the axion is left as a pseudo Goldstone boson. The corresponding current and their divergence are

$$\begin{aligned} J_{PQ}^\mu &= f_{a_1} \partial_\mu a_1 + m_1 \bar{Q} \gamma^\mu \gamma_5 Q + n_1 \bar{Q}' \gamma^\mu \gamma_5 Q', \\ J_{PQ'}^\mu &= f_{a_2} \partial_\mu a_2 + m_2 \bar{Q} \gamma^\mu \gamma_5 Q + n_2 \bar{Q}' \gamma^\mu \gamma_5 Q', \\ \partial_\mu J_{PQ}^\mu &= \frac{m_1 g^2}{16\pi^2} G_a^{\mu\nu} \tilde{G}_{a\mu\nu} + \frac{n_1 g'^2}{16\pi^2} G_A^{\mu\nu} \tilde{G}'_{A\mu\nu}, \\ \partial_\mu J_{PQ'}^\mu &= \frac{m_2 g^2}{16\pi^2} G_a^{\mu\nu} \tilde{G}_{a\mu\nu} + \frac{n_2 g'^2}{16\pi^2} G_A^{\mu\nu} \tilde{G}'_{A\mu\nu}, \end{aligned} \quad (7)$$

where  $G_a^{\mu\nu}$  and  $G_A^{\mu\nu}$  are strength tensors of gauge fields for QCD and hidden QCD, respectively.  $g$  and  $g'$  are couplings of the gauge interactions. In some papers, the hidden sector is extended to a ‘‘mirrored SM’’ with massive fermions  $u'$  and  $d'$  that do not carry  $U(1)_{PQ}$  charge like  $u$  and  $d$  in the SM [34,37].

The main structure of the dynamical solution [36] is shown in Fig. 1(b). As in the aligned axion model,  $SU(3)_h$  is introduced with a new  $CP$  parameter  $\theta'$ . Two massless fermions  $\psi$  and  $\chi$  are introduced to absorb  $CP$ -violating phases  $\theta$  and  $\theta'$  through a  $U(1)_A$  transformation. It is common to assume that  $SU(3)_h$  will confine just like QCD at a scale  $f_{\pi_h}$  which is much higher than the QCD confining scale  $f_\pi$ . The related currents are

$$\begin{aligned} J_A^\mu(\psi) &= \bar{\psi} \gamma^\mu \gamma_5 \psi, & J_A^\mu(\chi) &= \bar{\chi} \gamma^\mu \gamma_5 \chi, \\ \partial_\mu J_A^\mu(\psi) &= \frac{3g^2}{16\pi^2} F_a^{\mu\nu} \tilde{F}_{a\mu\nu} + \frac{3g'^2}{16\pi^2} G_A^{\mu\nu} \tilde{G}_{A\mu\nu}, \\ \partial_\mu J_A^\mu(\chi) &= \frac{g'^2}{16\pi^2} G_A^{\mu\nu} \tilde{G}_{A\mu\nu}. \end{aligned} \quad (8)$$

Below the scale  $f_{\pi_h}$ , we assume that the hidden sector has a dynamical chiral symmetry breaking caused by the fermion condensate with

$$\langle \bar{\psi} \psi \rangle \approx -c_\psi f_{\pi_h}^3, \quad \langle \bar{\chi} \chi \rangle \approx -c_\chi f_{\pi_h}^3, \quad (9)$$

where  $c_\psi, c_\chi$  are constants and  $f_{\pi_h} \gg f_\pi$ . Considering QCD as an additional ‘‘flavor symmetry,’’ there is an  $SU(4)_L \times SU(4)_R$  symmetry between  $\psi$  and  $\chi$ . After the condensate of hidden QCD,  $\pi_h^a$  are Goldstones corresponding to coset generators of  $SU(4)_L \times SU(4)_R / SU(4)_V$ . The decomposition of  $\pi_h^a$  into  $SU(3)_c$  is

$$15 = 8 + 3 + \bar{3} + 1. \quad (10)$$

The QCD color-singlet scalar is denoted as  $\pi_h \equiv \pi_h^{15}$  for short. The remainder of the 14 colored scalars are supposed to be heavy because of the QCD condensate. However, there is one more color-singlet scalar  $\eta'_h$  related to the  $U(1)_A$  symmetry. The corresponding currents related to these two fields are

$$\begin{aligned} J_\mu(\pi_h) &= \frac{1}{\sqrt{6}} (\bar{\psi}^c \gamma_\mu \gamma_5 \psi_c - 3 \bar{\chi} \gamma_\mu \gamma_5 \chi), \\ J_\mu(\eta'_h) &= \frac{1}{\sqrt{2}} (\bar{\psi}^c \gamma_\mu \gamma_5 \psi_c + \bar{\chi} \gamma_\mu \gamma_5 \chi), \end{aligned} \quad (11)$$

where  $c$  is the color index for  $\psi$ . These currents have been normalized, and we have chosen  $\text{tr}(T^a T^b) = 2\delta^{ab}$  as the normalization of the  $SU(4)$  generators. The specific matrices of  $SU(4)$  generators and details of derivation are shown in Appendix B. As a result of the condensate, we can use  $\pi_h$  and  $\eta'_h$  to represent the  $U(1)_A$  symmetry at the low energy scale.  $\theta$  and  $\theta'$  can be offset when  $\pi_h$  and  $\eta'_h$  take VEVs.

### III. CANCELLATION OF THE STRONG $CP$ PHASE

When one considers the extension of the SM, new contributions to the strong  $CP$  violation are introduced. Therefore, the strong  $CP$  phase  $\bar{\theta}$  needs to be modified. For distinction, the modified strong  $CP$  phase is notated as  $\theta_{\text{phy}}$ . In this section, we discuss these new contributions and methods to solve the strong  $CP$  problem. The difficulty is that  $\bar{\theta}$  is at order 1 but  $\theta_{\text{phy}}$  is at order  $10^{-10}$ . Axion models and dynamic solutions both solve this difficulty by cancelling  $\theta_{\text{phy}}$  at the minimal point of the Goldstone potential, which links  $\theta_{\text{phy}}$  with  $\bar{\theta}$ . To calculate  $\theta_{\text{phy}}$ , which describes  $CP$  violation effects at a scale lower than  $\Lambda_{\text{QCD}}$ , chiral perturbation theory (ChPT) is used to match fields of quarks with fields of hadrons. Indeed, it is sufficient to consider ChPT with two light quarks,  $u$  and  $d$ . The Lagrangian for QCD with an axion at hadron level is [41]

$$\begin{aligned} \mathcal{L}_2 &= \frac{f_\pi^2}{4} \text{Tr}(\partial_\mu U \partial^\mu U^\dagger) + A f_\pi^3 \text{Tr}(M U^\dagger + U M^\dagger) \\ &\quad - B f_\pi^4 \left( \theta + \frac{a}{f_a} + \frac{i}{2} \text{Tr}(\log U - \log U^\dagger) \right)^2, \end{aligned} \quad (12)$$

with

$$U = \exp \left[ \frac{i(\pi^a \tau^a + I\eta)}{f_\pi} \right], \quad M = \begin{pmatrix} m_u & 0 \\ 0 & m_d \end{pmatrix}, \quad (13)$$

where  $\pi^a$  and  $\eta$  are mesons and  $a$  is the axion.  $A$  and  $B$  are dimensionless parameters matched to the meson masses. Here  $\tau^a$  are Pauli matrices and  $I$  is the identity matrix. For convenience, we set the matrix of quark mass to be real in the rest of this paper, leading to  $\theta = \bar{\theta}$ . The potential part is shown as

$$V = -2Af_\pi^3 \left[ m_u \cos\left(\frac{\pi^0 + \eta}{f_\pi}\right) + m_d \cos\left(\frac{\pi^0 - \eta}{f_\pi}\right) \right] + Bf_\pi^4 \left( \frac{2\eta}{f_\pi} + \theta + \frac{a}{f_a} \right)^2. \quad (14)$$

For convenience,  $\langle \pi^0 \rangle / f_\pi$ ,  $\langle \eta \rangle / f_\pi$  and  $\langle a \rangle / f_a$  are defined as phases  $\phi_1$ ,  $\phi_2$ , and  $\phi_a$  respectively. Considering  $CP$  transformation,  $\pi^0$ ,  $\eta$ , and  $a$  are changed into  $-\pi^0$ ,  $-\eta$ , and  $-a$ . Once  $CP$  is conserved in Eq. (14), these phases need to meet

$$\phi_1 + \phi_2 = 0, \quad \phi_1 - \phi_2 = 0, \quad 2\phi_2 + \theta + \phi_a = 0, \quad (15)$$

which are equivalent to

$$\phi_1 = \phi_2 = 0, \quad \theta + \phi_a = 0. \quad (16)$$

Considering the derivative of the effective potential in Eq. (14) with respect to  $\pi^0$ ,  $\eta$ , and  $a$ , Eq. (16) is the exact solution at the minimal point of the potential. New contributions from  $U(1)$  symmetries are described by phase  $\phi_a$ . Finally, the  $CP$ -violating observable  $\theta_{\text{phy}}$  is derived as

$$\theta_{\text{phy}} = \theta + \phi_a = \theta + \frac{\langle a \rangle}{f_a}. \quad (17)$$

The strong  $CP$  problem is solved by the offset of axion VEV and the phase  $\theta$  to ensure  $\theta_{\text{phy}} = 0$ . Axion mass can also be derived from Eq. (14), following the procedure discussed in Appendix A, as

$$m_a^2 = m_\pi^2 \frac{f_\pi^2}{f_a^2} \frac{m_u m_d}{(m_u + m_d)^2}. \quad (18)$$

From this QCD axion model, it can be found that  $\theta_{\text{phy}}$  needs to be modified due to the new contribution of the axion. Similar absorption happens in other axion models and dynamical solutions.

For a general hidden QCD model with new fermions added, two UV free parameters,  $\theta$  and  $\theta'$ , have to be introduced. In general cases, the potential term induced by the instanton effect is

$$V_\theta = B_1 f_\pi^4 \left( \sum_{i=1}^2 m_i \frac{a_i}{f_{a_i}} + \theta \right)^2 + B_2 f_{\pi_h}^4 \left( \sum_{i=1}^2 n_i \frac{a_i}{f_{a_i}} + \theta' \right)^2, \quad (19)$$

where  $m$  and  $n$  stand for different anomalous charges.<sup>1</sup>

<sup>1</sup>It is more complex for dynamical solutions because the normalization factor also has to be included in this  $m$  and  $n$ .

Strong  $CP$  problems for both QCD and hidden QCD can be solved only by satisfying

$$\begin{aligned} \theta_{\text{phy}} &= \theta + \frac{\langle \eta' \rangle}{f_\pi} + \theta_{U(1)} = 0, \\ \theta'_{\text{phy}} &= \theta' + \theta'_{U(1)} = 0. \end{aligned} \quad (20)$$

In Eq. (20),  $\langle \eta' \rangle$  represents the contribution of the VEV of  $\eta'$ , which can be absorbed by redefinition of  $\theta$ . We are not interested in this, so we will include it with  $\theta$  in the following discussion.  $\theta_{U(1)}$  and  $\theta'_{U(1)}$  come from the axion VEVs. In the following subsections, we discuss the  $\theta$  cancellation of Eq. (20) in some specific models with different  $U(1)$  symmetries.

### A. One $U(1)$

As shown in Eq. (20), there are 2 degrees of freedom needed to absorb both  $\theta$  and  $\theta'$ . When only one  $U(1)$  is introduced, there is only 1 new degree of freedom. This means that  $\theta$  and  $\theta'$  cannot be absorbed simultaneously and the strong  $CP$  problem cannot be solved. To solve this problem, a mirrored  $Z_2$  symmetry has to be introduced between  $SU(3)_c$  in the SM and  $SU(3)_h$  in the hidden sector. In UV theories, some models can achieve this by embedding these two  $SU(3)$  in a larger gauge symmetry group  $SU(6)$  [37]. Consequently, two  $CP$  phases are forced to be identical, which means that

$$\theta = \theta'. \quad (21)$$

As shown in Fig. 2, the additional  $U(1)$  could be achieved using two methods. One method introduces an axion with  $U(1)_{PQ}$  [Fig. 2(a)] and the other uses massless  $\psi(3, 3)$  with  $U(1)_A$  [Fig. 2(b)]. There are detailed discussions about both methods in the literature [24,31–35]. In Fig. 2(a), the cancellation equation (20) becomes

$$\theta'_{\text{phy}} = \theta_{\text{phy}} = \theta + \frac{\langle a \rangle}{f_a} = 0. \quad (22)$$

In Fig. 2(b), as shown in Appendix B, the cancellation equation (20) is deduced as

$$\theta'_{\text{phy}} = \theta_{\text{phy}} = \theta + \sqrt{6} \frac{\langle \eta'_h \rangle}{f_{\pi_h}} = 0. \quad (23)$$

In both cases, the strong  $CP$  problem is solved by only one  $U(1)$  symmetry, and the  $CP$ -violating effects from  $\theta$  and  $\theta'$  are counteracted by  $\langle a \rangle$  or  $\langle \eta'_h \rangle$ .

### B. Two similar $U(1)$ 's

As in the previous subsection, models with two  $U(1)$  freedoms can be sorted by different mechanisms of  $U(1)$  symmetries. As shown in Fig. 1, models could contain two

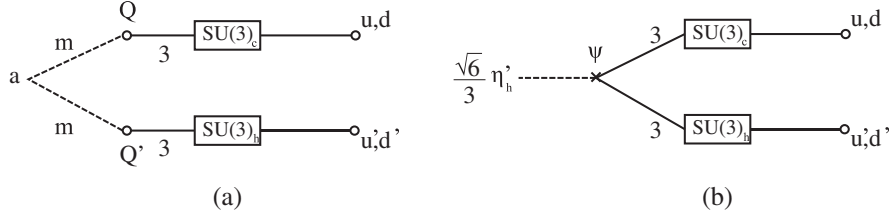


FIG. 2. (a) Structure of  $U(1)_{PQ}$  models with mirror symmetry. (b) Structure of  $U(1)_A$  dynamic solutions with mirror symmetry.

$U(1)_{PQ}$  or two  $U(1)_A$  symmetries. For these kinds of models, axial currents are determined by representations of fermions in  $SU(3)_c$  and  $SU(3)_h$ . The cancellation equation of  $\theta$  and  $\theta'$  will be determined by these currents and different  $U(1)$  charge for fermions.

Here we see another advantage of our diagram method that the cancellation equation can be read easily. Figure 1(a) shows models with two  $U(1)_{PQ}$  symmetries. Choosing  $SU(3)_c$  as the starting point responsible for  $\theta$ , we can find that all possible links end on the left side. Notice that these links can only go from right to left. The canceling phase of each link is the product of the charge number on the dashed line and the scale factor at the end point on the left. Finally, we can sum all offset terms from different links together. For  $\theta'$ , the starting point will be changed into  $SU(3)_h$ , and we then repeat these steps. The cancellation equations from our diagram read

$$\begin{aligned}\theta_{\text{phy}} &= \theta + m_1 \frac{\langle a_1 \rangle}{f_{a_1}} + m_2 \frac{\langle a_2 \rangle}{f_{a_2}} = 0, \\ \theta'_{\text{phy}} &= \theta' + n_1 \frac{\langle a_1 \rangle}{f_{a_1}} + n_2 \frac{\langle a_2 \rangle}{f_{a_2}} = 0.\end{aligned}\quad (24)$$

This two-axion model has been widely discussed. When the angle between vectors  $(m_1, m_2)$  and  $(n_1, n_2)$  is near zero (but not zero), in contrast to large  $m$  and  $n$ , it is exactly the ‘‘alignment axion’’ model [20,21].

Models with two  $U(1)_A$  symmetries provided by massless fermions have similar expressions for  $CP$ -violating angles. In Fig. 1(b),  $M_\psi = 0$  and  $M_\chi = 0$  are assumed. The corresponding currents are given in Eq. (11). It is a bit more complex to read cancellation equations for this model from the figure. There are two other things to notice. First, the normalization factor has already been written, together with the scale factor. Second, the degeneracy, which comes from the color index of the other  $SU(3)$  outside the link, should be multiplied by each link. The degeneracy can be read from the number for representation on other solid lines attached to the fermion field. For example, the degeneracy of the link, ‘‘ $SU(3)_c \rightarrow \psi \rightarrow \pi_h$ ,’’ will be the number 3 on the solid line attached to  $\psi$  and  $SU(3)_h$ . When we sum all links together, this link should be multiplied by 3. The final cancellation equations are

$$\begin{aligned}\theta_{\text{phy}} &= \theta + \frac{\sqrt{6}}{2} \frac{\langle \pi_h \rangle}{f_h} + \frac{3\sqrt{2}}{2} \frac{\langle \eta'_h \rangle}{f_h} = 0, \\ \theta'_{\text{phy}} &= \theta' + 2\sqrt{2} \frac{\langle \eta'_h \rangle}{f_h} = 0.\end{aligned}\quad (25)$$

The cancellation equations of other figures can also be read in this way.

### C. Two different $U(1)$ 's

In these two- $U(1)$  solutions,  $U(1)$ 's need not to be the same, which means that models of one  $U(1)_{PQ}$  and one  $U(1)_A$  are possible. Here we show two simple examples of these new kinds of models in Fig. 3.

The mixed solution of  $U(1)_{PQ}$  and  $U(1)_A$  would be more complex, for the reason that two independent scales,  $f_h$  and  $f_a$ , are simultaneously involved.  $f_h$  is the condensate scale of the hidden QCD fermions, while  $f_a$  is the spontaneously breaking scale of the Peccei-Quinn symmetry. Figure 3(a) shows model A, in which  $U(1)_{PQ}$  is spontaneously broken independently of the hidden QCD. The result of the cancellation equations in this model is

$$\begin{aligned}\theta_{\text{phy}} &= \theta + \sqrt{6} \frac{\langle \eta'_h \rangle}{f_h} + m \frac{\langle a \rangle}{f_a} = 0, \\ \theta'_{\text{phy}} &= \theta' + \sqrt{6} \frac{\langle \eta'_h \rangle}{f_h} + n \frac{\langle a \rangle}{f_a} = 0.\end{aligned}\quad (26)$$

Figure 3(b) shows model B, in which the spontaneous breaking of  $U(1)_{PQ}$  is induced by the hidden QCD. The cancellation equations are

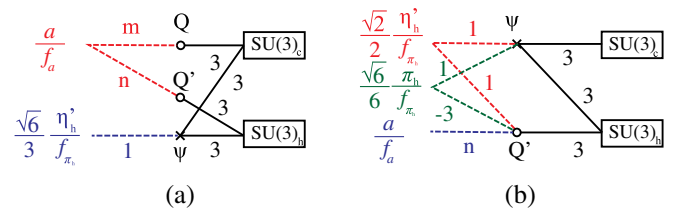


FIG. 3. Structure of models with mixed  $U(1)$ s. (a) Model A. The spontaneous breaking of  $U(1)_{PQ}$  is independent of the hidden QCD. (b) Model B. The dynamical symmetry breaking of hidden QCD induces  $U(1)_{PQ}$  breaking.

$$\begin{aligned}\theta_{\text{phy}} &= \theta + \frac{3}{\sqrt{2}} \frac{\langle \eta'_h \rangle}{f_h} + \frac{3}{\sqrt{6}} \frac{\langle \pi_h \rangle}{f_h} = 0, \\ \theta'_{\text{phy}} &= \theta' + 2\sqrt{2} \frac{\langle \eta'_h \rangle}{f_h} + n \frac{\langle a \rangle}{f_a} = 0.\end{aligned}\quad (27)$$

It seems that redundancy exists in these equations, as there are three VEVs to absorb two  $\theta$  parameters. However, there is an additional equation constraining these three VEVs from the Yukawa term of  $Q'$ , as shown in Eq. (62) in the next section.

#### IV. PHYSICAL OBSERVABLES

In this section, we study the most important physical observables, axion mass and axion-photon coupling in the one-axion solution and mixed two-axion solutions, which cannot be directly obtained from diagrams in the last section.

The relevant Lagrangian that parametrizes the coupling  $g_{a\gamma\gamma}$  between the physical axion and photon is defined as [42]

$$\mathcal{L}_{a\gamma\gamma} = \frac{1}{4} g_{a\gamma\gamma} a F_{\mu\nu} \tilde{F}^{\mu\nu} = \frac{1}{4} (g_{a\gamma\gamma}^{\text{IR}} + g_{a\gamma\gamma}^{\text{UV}}) a F_{\mu\nu} \tilde{F}^{\mu\nu}. \quad (28)$$

Here the physical axion could be the lightest states coming from the mixing of multiple pseudo Goldstones of different anomalous  $U(1)$  symmetries in the UV. The coupling  $g_{a\gamma\gamma}^{\text{IR}}$  is generated by the mixing between physical axion  $a$  and QCD mesons through the potential in Eq. (14), and up to NLO accuracy [42] it is

$$g_{a\gamma\gamma}^{\text{IR}} = -1.92(4) \frac{\alpha_{\text{em}}}{2\pi F_a}, \quad (29)$$

with the decay constant  $F_a$  [effectively  $f_a$  in Eq. (14)] defined by the axion-gluon anomalous coupling:  $\frac{a}{F_a} \frac{g_s^2}{32\pi^2} G_{\mu\nu} \tilde{G}^{\mu\nu}$ . The  $g_{a\gamma\gamma}^{\text{UV}}$  is the contribution from UV originating from the electromagnetic anomaly of axions, which varies from model to model. In the ordinary QCD axion model like KSVZ and DFSZ, it is simply given by [43]

$$g_{a\gamma\gamma}^{\text{UV}} = \frac{E}{N} \frac{\alpha_{\text{em}}}{2\pi F_a}, \quad (30)$$

where  $E$  and  $N$  are, respectively, the electromagnetic and color anomaly coefficients determined by the properties of fermions contributing to the anomaly triangle diagrams. In Secs. IV B 1 and IV B 2, we illustrate the forms of the  $g_{a\gamma\gamma}^{\text{UV}}$  for the two new two-axion models proposed by us, where we show that the key point to derive the axion-photon couplings is to find the mixing coefficients of the lightest physical axion in terms of those pseudo Goldstones of  $U(1)$ 's and (hidden) QCD mesons,

which are obtained by diagonalizing the mass matrix of these mixed states.

For the other physical observable, the axion mass, we find that, in the models with only one axion with an extended hidden QCD sector, the mass of the axion is always enhanced by the condensate of the hidden QCD, while for the two-axion solutions, a light axion (similar to the mass scale of the ordinary QCD axion) always exists.

#### A. One-axion solution

The one-axion solution is the exact implementation of the visible axion model, in which the axion mass is enhanced by the condensate scale of the hidden QCD. We illustrate this with a specific model shown in Fig. 2(a). The Lagrangian can be written as

$$\Delta\mathcal{L} = g f_a e^{i2ma/f_a} \bar{Q}_L Q_R + g' f_a e^{i2ma/f_a} \bar{Q}'_L Q'_R + \text{H.c.}, \quad (31)$$

where  $a$  is a pseudoscalar and  $f_a$  is a scale factor. The UV completion of Lagrangian (31) can be implemented by the clockwork mechanism [44]. There is a  $U(1)_{PQ}$  to keep the Lagrangian invariant under transformations:

$$a/f_a \rightarrow a/f_a + \alpha, \quad Q \rightarrow e^{i\gamma_5 m \alpha} Q, \quad Q' \rightarrow e^{i\gamma_5 m \alpha} Q'. \quad (32)$$

Assuming a mirrored  $Z_2$  symmetry between the SM and the hidden sector, in this model a single  $U(1)_{PQ}$  chiral symmetry is enough to solve the strong  $CP$  problem. The corresponding current of  $U(1)_{PQ}$  and its divergence are

$$\begin{aligned}J_{PQ}^\mu &= f_a \partial_\mu a + m \bar{Q} \gamma^\mu \gamma_5 Q + m \bar{Q}' \gamma^\mu \gamma_5 Q', \\ \partial_\mu J_{PQ}^\mu &= \frac{mg^2}{16\pi^2} F_a^{\mu\nu} \tilde{F}_{a\mu\nu} + \frac{mg'^2}{16\pi^2} G_A^{\mu\nu} \tilde{G}_{A\mu\nu}.\end{aligned}\quad (33)$$

At the low energy scale, the axion mass term stems from the instanton effects of QCD and hidden QCD. As in Eq. (14), the potentials of the axion, pions, and hidden pions are

$$\begin{aligned}V &= -2A f_\pi^3 \left[ m_u \cos\left(\frac{\pi^0 + \eta}{f_\pi}\right) + m_d \cos\left(\frac{\pi^0 - \eta}{f_\pi}\right) \right] \\ &\quad + B f_\pi^4 \left( \frac{2\eta}{f_\pi} + \theta + \frac{ma}{f_a} \right)^2 \\ &\quad - 2A' f_{\pi_h}^3 \left[ m_{u'} \cos\left(\frac{\pi_h^0 + \eta_h}{f_{\pi_h}}\right) + m_{d'} \cos\left(\frac{\pi_h^0 - \eta_h}{f_{\pi_h}}\right) \right] \\ &\quad + B' f_{\pi_h}^4 \left( \frac{2\eta_h}{f_{\pi_h}} + \theta + \frac{ma}{f_a} \right)^2,\end{aligned}\quad (34)$$

where  $u'$  and  $d'$  are mirrored quarks. The  $\theta$  angle can be absorbed by an axion at the minimal point of the potential.

Because  $f_{\pi_h} \gg f_\pi$ , the contributions to the axion masses of the first and second terms are negligible. If we assume that  $f_a \gg f_{\pi_h}$ , integrating out  $\eta_h$  with the procedure discussed in Appendix A, the potential of Eq. (34) to leading order (simply omitting the entire dependence of the heavy fields) becomes

$$V = -2A'f_{\pi_h}^3 \left[ m_{u'} \cos\left(\frac{\pi_h^0}{f_{\pi_h}} - \frac{a}{2F_a}\right) + m_{d'} \cos\left(\frac{\pi_h^0}{f_{\pi_h}} + \frac{a}{2F_a}\right) \right], \quad (35)$$

where  $F_a = f_a/m$ . Diagonalizing the mass matrix of  $\pi_h^0$  and  $a$ , the mass of the axion is

$$m_a = \frac{m_{\pi_h} f_{\pi_h}}{F_a} \frac{\sqrt{m_{u'} m_{d'}}}{(m_{u'} + m_{d'})}, \quad (36)$$

where  $m_{\pi_h}^2 = 2A'f_{\pi_h}(m_{u'} + m_{d'})$ . The axion mass could be much heavier than the KSVZ and DFSZ axions. Different phenomena of the heavy axion may appear in collider experiments or rare decay of the mesons [37].

## B. Two-axion solutions

In two-axion solutions with extra hidden QCD, the light mass eigenstate always exists and can be treated as an invisible axion, even if  $\Lambda_h = 4\pi f_{\pi_h}$  is much higher than the QCD scale  $\Lambda_c = 4\pi f_\pi$ . We illustrate our claims for the axion mass in general scenarios with two light hidden quarks in the hidden QCD sector, then derive masses and axion-photon couplings for the two concrete UV models in Secs. IV B 1 and IV B 2 corresponding to the two figures listed in Fig. 3.

We assume that two light hidden quarks ( $u'$  and  $d'$ ) exist in the hidden sector, which is similar to the SM. The potential of axions, mesons, and hidden bosons are

$$V = -2A'f_\pi^3 \left[ m_u \cos\left(\frac{\pi^0 + \eta}{f_\pi}\right) + m_d \cos\left(\frac{\pi^0 - \eta}{f_\pi}\right) \right] + B'f_\pi^4 \left( \frac{2\eta}{f_\pi} + \theta + \frac{m_1 a_1}{f_{a_1}} + \frac{m_2 a_2}{f_{a_2}} \right)^2 - 2A'f_{\pi_h}^3 \left[ m_{u'} \cos\left(\frac{\pi_h^0 + \eta_h}{f_{\pi_h}}\right) + m_{d'} \cos\left(\frac{\pi_h^0 - \eta_h}{f_{\pi_h}}\right) \right] + B'f_{\pi_h}^4 \left( \frac{2\eta_h}{f_{\pi_h}} + \theta' + \frac{n_1 a_1}{f_{a_1}} + \frac{n_2 a_2}{f_{a_2}} \right)^2, \quad (37)$$

where  $f_{a_1}$  and  $f_{a_2}$  are scale factors. Anomaly coefficients of axions are denoted as  $m_1, m_2, n_1$ , and  $n_2$ . The  $CP$  angles  $\theta$  and  $\theta'$  can be absorbed by  $a_1$  and  $a_2$  at the minimal point of potential. Since  $f_{\pi_h} \gg f_\pi$ , the terms with respect to  $f_\pi$  can be treated as perturbed. First, we focus on the heavy degree of freedom. The potential of axions and hidden bosons

$$V_h = -2A'f_{\pi_h}^3 \left[ m_{u'} \cos\left(\frac{\pi_h^0 + \eta_h}{f_{\pi_h}}\right) + m_{d'} \cos\left(\frac{\pi_h^0 - \eta_h}{f_{\pi_h}}\right) \right] + B'f_{\pi_h}^4 \left( \frac{2\eta_h}{f_{\pi_h}} + \theta' + \frac{n_1 a_1}{f_{a_1}} + \frac{n_2 a_2}{f_{a_2}} \right)^2. \quad (38)$$

As in the discussion in Sec. IV A, if we assume that  $f_{a_1}, f_{a_2} \gg f_{\pi_h}$ , integrating out the much heavier state that mainly consists of  $\eta_h$  leads to an effective potential mixing  $\pi_h^0$  and the remaining two light axions:

$$V_{\text{eff}} = -2A'f_{\pi_h}^3 \left[ m_{u'} \cos\left(\frac{\pi_h^0}{f_{\pi_h}} - \frac{n_1 a_1}{f_{a_1}} - \frac{n_2 a_2}{f_{a_2}}\right) + m_{d'} \cos\left(\frac{\pi_h^0}{f_{\pi_h}} + \frac{n_1 a_1}{f_{a_1}} + \frac{n_2 a_2}{f_{a_2}}\right) \right]. \quad (39)$$

One can identify that the heavier axion is denoted as

$$A \propto \frac{n_1 a_1}{f_{a_1}} + \frac{n_2 a_2}{f_{a_2}}, \quad (40)$$

where we have neglected the  $\eta_h$  and  $\pi_h$  components of  $A$  which are suppressed by  $f_{\pi_h}/\sqrt{f_{a_1}^2 + f_{a_2}^2}$ .<sup>2</sup> The mass of  $A$  is given as

$$m_A = \frac{m_{\pi_h} f_{\pi_h}}{F_A} \frac{\sqrt{m_{u'} m_{d'}}}{(m_{u'} + m_{d'})} \sim f_{\pi_h}^2 / F_A, \quad (41)$$

where  $F_A$  is the decay constant of heavy axion  $A$ , and again  $m_{\pi_h}^2 = 2A'f_{\pi_h}(m_{u'} + m_{d'})$ . The massless one is in the orthogonal direction with  $A$  in field space, which is

$$a \propto \frac{n_2 a_1}{f_{a_2}} - \frac{n_1 a_2}{f_{a_1}}. \quad (42)$$

Replacing  $(a_1, a_2)$  with  $(A, a)$  and integrating out the heavy particles  $\pi_h^0, \eta_h'$ , and  $A$ , to leading order Eq. (37) becomes

<sup>2</sup>These suppressed components of  $\pi_h$  and  $\eta_h$  are important for axion-photon couplings but do not affect our derivation of the mass parameters to leading order accuracy. In model A,  $\psi$  is massless; therefore, axions have no mixing with  $\pi_h$ . In model B,  $\psi$  is massless and  $Q'$  is a light hidden quark; therefore, axions have a mixing with  $\pi_h$ .<sup>15</sup>

$$V_{\text{IR}} = -2A f_\pi^3 \left[ m_u \cos\left(\frac{\pi^0 + \eta}{f_\pi}\right) + m_d \cos\left(\frac{\pi^0 - \eta}{f_\pi}\right) \right] + B f_\pi^4 \left( \frac{2\eta}{f_\pi} + \frac{a}{F_a} \right)^2, \quad (43)$$

where  $F_a$  is the decay constant of the light axion. The mass of the light axion is the same invisible QCD axion found in Eq. (18),

$$m_a = \frac{m_\pi f_\pi}{F_a} \frac{\sqrt{m_u m_d}}{(m_u + m_d)^2}. \quad (44)$$

Up to now we have demonstrated the existence of a light axion with a conventional QCD axion mass scale

in the two axion models with an extended hidden QCD structure.

In the following section, we discuss two specific models with different breaking mechanisms in mixed two-axion solutions. The model with two independently breaking  $U(1)$  symmetries (model A) is shown in Fig. 3(a) with masses of  $Q$  and  $Q'$  larger than  $\Lambda_h$ , and the model with one breaking  $U(1)$  symmetry induced by the other (model B) is shown in Fig. 3(b) with masses of  $Q'$  lighter than  $\Lambda_h$ . For simplicity,  $Q$  is not introduced in model B. The main difference between these two models is whether the symmetry breaking of  $U(1)_{PQ}$  is induced by the breaking of  $U(1)_A$ . Chiral symmetries are the same in both cases. The corresponding currents and the divergence of these models are

$$\begin{aligned} J_A^\mu &= \frac{\sqrt{6}}{3} \bar{\psi} \gamma^\mu \gamma_5 \psi, & J_{PQ}^\mu &= f_{a_1} \partial_\mu a_1 + (m \bar{Q} \gamma^\mu \gamma_5 Q) + n \bar{Q}' \gamma^\mu \gamma_5 Q', \\ \partial_\mu J_A^\mu &= \frac{\sqrt{6} g^2}{16\pi^2} G_a^{\mu\nu} \tilde{G}_{a\mu\nu} + \frac{\sqrt{6} g^2}{16\pi^2} G_A^{\mu\nu} \tilde{G}'_{A\mu\nu}, \\ \partial_\mu J_{PQ}^\mu &= \frac{m g^2}{16\pi^2} G_a^{\mu\nu} \tilde{G}_{a\mu\nu} + \frac{n g^2}{16\pi^2} G_A^{\mu\nu} \tilde{G}'_{A\mu\nu}, \end{aligned} \quad (45)$$

where we set the anomaly coefficient  $m = 0$  in the second model for simplicity.

### 1. Model A

In model A, the spontaneous breaking of two chiral  $U(1)$  symmetries comes from different mechanisms. The  $U(1)_{PQ}$  symmetry is broken by the effective potential of the complex scalar  $\phi$ , while  $U(1)_A$  is broken by the condensate of the massless fermion  $\psi$ . Therefore, these two breaking scales are independent, and the Goldstones associated with these two anomalous  $U(1)$  symmetries serve as two axions. The only source of explicit breaking comes from the instanton effects contributing to the masses of both axions.

The mass-relevant Lagrangian in the following equation consists of three parts, the mass term for QCD mesons  $\pi^0$  and  $\eta$  in chiral perturbation theory and the instanton effects from both QCD and hidden QCD:

$$\begin{aligned} -\mathcal{L}_{\text{mass}} &= \dots - 2A f_\pi^3 \left[ m_u \cos\left(\frac{\pi^0 + \eta}{f_\pi}\right) + m_d \cos\left(\frac{\pi^0 - \eta}{f_\pi}\right) \right] + B f_\pi^4 \left( \frac{2\eta}{f_\pi} + \frac{\sqrt{6}\eta'_h}{f_{\pi_h}} + \frac{m a_1}{f_{a_1}} \right)^2 \\ &+ B' f_{\pi_h}^4 \left( \frac{\sqrt{6}\eta'_h}{f_{\pi_h}} + \frac{n a_1}{f_{a_1}} \right)^2. \end{aligned} \quad (46)$$

The only nontrivial parts are the last two terms from the instanton effects. The coefficients of  $\eta'_h$  and  $a_1$  are read from Eq. (45), where  $\eta'_h$  is associated with  $J_A^\mu$  and  $a_1$  is associated with  $J_{PQ}^\mu$ . The divergences of these currents indicate that both  $\eta'_h$  and  $a_1$  get corrections from QCD and hidden QCD instanton effects, and the coefficients of  $\eta'_h$  and  $a_1$  in Eq. (46) are obtained by the matching [43] since the second (third) term stems from QCD (hidden QCD) instanton effects with  $f_{\pi_h} \gg f_\pi$ . The mass matrix of  $(\pi^0, \eta, \eta'_h, a_1)$  can be written as

$$\begin{pmatrix} M_\pi & A \\ A^T & M_{\pi_h} \end{pmatrix} = \begin{pmatrix} 0 & 0 \\ 0 & M_{\pi_h} \end{pmatrix} + \begin{pmatrix} M_\pi & A \\ A^T & 0 \end{pmatrix}, \quad (47)$$

where  $M_\pi$ ,  $A$ ,  $M_{\pi_h}$  are  $2 \times 2$  submatrices.  $M_\pi$  and  $A$  come from the first and second terms of Eq. (46), respectively, and  $M_{\pi_h}$  comes from the second and third terms. Owing to the fact that  $f_{\pi_h} \gg f_\pi$ , the elements of  $M_{\pi_h}$  are much larger than the elements of  $M_\pi$  and  $A$ ; therefore, one can diagonalize  $M_{\pi_h}$  in the subspace of  $\eta'$  and  $a_1$  first and then treat the remaining parts as a perturbation.

After diagonalizing the  $M_{\pi_h}$  matrix, there will be two mass eigenstates. The lighter mass eigenstate  $a$  is

$$a = \frac{nf_{\pi_h}\eta'_h - \sqrt{6}f_{a_1}a_1}{\sqrt{6f_{a_1}^2 + n^2f_{\pi_h}^2}}. \quad (48)$$

The heavier mass eigenstate can be integrated out and has a negligible effect in the IR region. After we integrate out the heavy axion, the remaining parts of the mass matrix are similar to Eq. (14), with  $f_a$  changed to  $F_a = \sqrt{6f_{a_1}^2 + n^2f_{\pi_h}^2}/(\sqrt{6}|m-n|)$ . Next, diagonalizing the remaining mass matrix for  $(\pi^0, \eta, a)$ , the axion mass is obtained as

$$m_a^2 F_a^2 = m_\pi^2 f_\pi^2 \frac{m_u m_d}{(m_u + m_d)^2}. \quad (49)$$

In model A,  $g_{a\gamma\gamma}^{\text{UV}}$  is generated from the mixing of  $\eta'_h$  and  $a_1$ . The anomaly-induced interactions between  $\eta'_h$ ,  $a_1$ , and the photon can be written as

$$\mathcal{L}_{a\gamma\gamma} = \left( 3\sqrt{6}q_\psi^2 \frac{\eta'_h}{f_{\pi_h}} + 3(mq_Q^2 + nq_{Q'}^2) \frac{a_1}{f_{a_1}} \right) \frac{\alpha_{\text{em}}}{4\pi} F_{\mu\nu} \tilde{F}^{\mu\nu}, \quad (50)$$

where  $q_\psi$ ,  $q_Q$ , and  $q_{Q'}$  denote the electric charge of each particles. Therefore, we can obtain  $g_{a\gamma\gamma}^{\text{UV}}$  according to Eq. (48),

$$g_{a\gamma\gamma}^{\text{UV}} = \frac{6n(q_\psi^2 - q_{Q'}^2) - 6mq_Q^2}{|m-n|} \frac{\alpha_{\text{em}}}{2\pi F_a}. \quad (51)$$

When setting  $n \gg |m-n|$ , the UV contribution of the axion-photon coupling is enlarged. Meanwhile, the physical axion decay constant meets the condition  $F_a \gg f_{a_1}$ , as shown in Eq. (49), which enables the model to solve the axion quality problem. This result is actually a special case of ‘‘alignment axion’’ models [20,21].

## 2. Model B

This model contain massless fermion  $\psi$  charged under both QCD and hidden QCD, a fermion  $Q'$  charged under only hidden QCD with a complex scalar  $\phi$ . Their transformation properties under the  $U(1)_{PQ}$  are

$$\phi \rightarrow e^{i\alpha}\phi, \quad \psi \rightarrow \psi, \quad Q' \rightarrow e^{i\gamma_5 m\alpha} Q'. \quad (52)$$

The Lagrangian of this model can be written as

$$\begin{aligned} \Delta\mathcal{L} = & i\bar{\psi}D_{1\mu}\gamma^\mu\psi + i\bar{Q}'D_{2\mu}\gamma^\mu Q' + (y\phi\bar{Q}'_L Q'_R + \text{H.c.}) \\ & + \partial_\mu\phi\partial^\mu\phi^* - \mu^2\phi^2, \end{aligned} \quad (53)$$

where

$$D_{1\mu} = \partial_\mu + iG_\mu^a T^a + iG_\mu'^A T^A, \quad D_{2\mu} = \partial_\mu + iG_\mu'^A T^A, \quad (54)$$

and where there is only a light fermion  $Q'$ . The corresponding currents of  $U(1)_A$  and  $U(1)_{PQ}$  are

$$\begin{aligned} J_A^\mu &= \frac{\sqrt{6}}{3} \bar{\psi}\gamma^\mu\gamma_5\psi, \\ J_{PQ}^\mu &= (\phi i\partial_\mu\phi^* - \phi^* i\partial_\mu\phi) + \bar{Q}'\gamma^\mu\gamma_5 Q', \end{aligned} \quad (55)$$

where the anomaly coefficient of  $Q'$  is  $n=1$ . We are particularly interested in the case where the spontaneous breaking of  $U(1)_{PQ}$  is triggered by the condensate of the light fermion  $Q'$  in the hidden sector such that the two breaking scales are related. We assume the potential of the complex scalar  $\phi$  containing only a quadratic term with  $\mu^2 > 0$ , and the Yukawa term of  $Q'$  will induce a tadpole term of  $\phi$  after the chiral symmetry breaking in the hidden sector. The Lagrangian after the chiral symmetry breaking is

$$\begin{aligned} \mathcal{L}_{\text{CSB}} = & \partial_\mu\phi\partial^\mu\phi^* - \mu^2\phi^2 + \frac{f_{\pi_h}^2}{4} \text{Tr}\partial_\mu\Sigma\partial^\mu\Sigma^\dagger \\ & + A'f_{\pi_h}^3 \text{Tr}(H\Sigma^\dagger + H^\dagger\Sigma) \\ & - B'f_\pi^4 \left( \theta' + \frac{i}{2} \text{Tr}(\log\Sigma - \log\Sigma^\dagger) \right)^2, \end{aligned} \quad (56)$$

where

$$\Sigma = \exp\left[\frac{i(\pi_h^a T^a + \frac{1}{\sqrt{2}}I_{4\times 4}\eta'_h)}{f_\pi}\right], \quad H = \begin{pmatrix} 0 & & & \\ & 0 & & \\ & & 0 & \\ & & & y\phi \end{pmatrix}. \quad (57)$$

Here  $T^a$  are generators of the  $SU(4)$  group meeting the trace condition  $\text{Tr}(T^a T^b) = 2\delta^{ab}$ . The anomalous term is omitted in Eq. (56). The Yukawa coupling matrix  $H$  of  $\psi$  and  $Q'$  is treated as a spurion field, transforming to an adjoint representation under the  $SU(4)_V$ . The third term in Eq. (56) is the linear term of  $\phi$  which triggers  $U(1)_{PQ}$  breaking. The effective potential of  $\phi$  and  $\Sigma$  is given by

$$\begin{aligned} V(\phi, \Sigma) = & \mu^2\phi^2 - A'f_{\pi_h}^3 \left[ y\phi \exp\left(i\frac{-\frac{3}{\sqrt{6}}\pi_h^{15} + \frac{1}{\sqrt{2}}\eta'_h}{f_\pi}\right) + \text{H.c.} \right] \\ & + B'f_{\pi_h}^4 \left( \theta' + \frac{2\sqrt{2}\eta'_h}{f_{\pi_h}} \right)^2. \end{aligned} \quad (58)$$

The VEV of  $\phi$  is estimated as

$$\langle |\phi| \rangle \lesssim 2y \frac{A'f_{\pi_h}^3}{\mu^2}, \quad (59)$$

and the complex scalar  $\phi$  can be parametrized as

$$\phi = \frac{1}{\sqrt{2}}(\rho + f_{a_1})e^{i\frac{a_1}{f_{a_1}}}, \quad (60)$$

with  $f_{a_1}/\sqrt{2} = \langle |\phi| \rangle \lesssim 2yA'f_{\pi_h}^3/\mu^2$ . The coefficients of  $\pi_h^{15}$  and  $\eta'_h$  in the  $f_\pi^4$  term in the IR QCD potential from the instanton effect can be determined by the corresponding currents and their divergence:

$$\begin{aligned} J^\mu(\eta_h) &= \frac{1}{\sqrt{2}}(\bar{\psi}\gamma^\mu\gamma_5\psi + \bar{Q}'\gamma^\mu\gamma_5Q'), & J^\mu(\pi_h^{15}) &= \frac{1}{\sqrt{6}}(\bar{\psi}\gamma^\mu\gamma_5\psi - 3\bar{Q}'\gamma^\mu\gamma_5Q'), \\ \partial_\mu J^\mu(\eta_h) &= \frac{3\sqrt{2}}{2}\frac{g^2}{16\pi^2}G_a^{\mu\nu}\tilde{G}_{a\mu\nu} + \frac{2\sqrt{2}g^2}{16\pi^2}G_A^{\mu\nu}\tilde{G}'_{A\mu\nu}, \\ \partial_\mu J^\mu(\pi_h^{15}) &= \frac{3}{\sqrt{6}}\frac{g^2}{16\pi^2}G_a^{\mu\nu}\tilde{G}_{a\mu\nu}. \end{aligned} \quad (61)$$

Therefore, the mass terms of the scalars in Lagrangian (56) (QCD sector contained) become

$$\begin{aligned} -\mathcal{L}_{\text{mass}} &= -2Af_\pi^3 \left[ m_u \cos\left(\frac{\pi^0 + \eta}{f_\pi}\right) + m_d \cos\left(\frac{\pi^0 - \eta}{f_\pi}\right) \right] + Bf_\pi^4 \left[ \frac{2\eta}{f_\pi} + \sqrt{6} \left( \frac{1}{2} \frac{\pi_h^{15}}{f_{\pi_h}} + \frac{\sqrt{3}}{2} \frac{\eta'_h}{f_{\pi_h}} \right) \right]^2 \\ &+ A'y \frac{f_{a_1}f_{\pi_h}^3}{\sqrt{2}} \left( \frac{a_1}{f_{a_1}} - \frac{3}{\sqrt{6}} \frac{\pi_h^{15}}{f_{\pi_h}} + \frac{1}{\sqrt{2}} \frac{\eta'_h}{f_{\pi_h}} \right)^2 + B'f_{\pi_h}^4 \left( \frac{2\sqrt{2}\eta'_h}{f_{\pi_h}} \right)^2. \end{aligned} \quad (62)$$

The  $a_1/f_{a_1}$  in the third term could move to the fourth term using a chiral rotation  $\theta' \rightarrow \theta' + a_1/f_{a_1}$  and generates an additional differential interaction of  $a_1$ . By means of the same steps in the Sec. IV B 2, we first treat the terms relevant to the heavy degrees of freedom in the space of  $(a_1, \pi_h^{15}, \eta'_h)$  as  $f_{\pi_h} \gg f_\pi$ :

$$-\delta\mathcal{L}_{\text{mass}} = A'y \frac{f_{a_1}f_{\pi_h}^3}{\sqrt{2}} \left( \frac{a_1}{f_{a_1}} - \frac{3}{\sqrt{6}} \frac{\pi_h^{15}}{f_{\pi_h}} + \frac{1}{\sqrt{2}} \frac{\eta'_h}{f_{\pi_h}} \right)^2 + B'f_{\pi_h}^4 \left( \frac{2\sqrt{2}\eta'_h}{f_{\pi_h}} \right)^2. \quad (63)$$

Diagonalizing the  $3 \times 3$  matrix yields a massless scalar is

$$a = \frac{f_{\pi_h}\pi_h^{15} + 3/\sqrt{6}f_{a_1}a_1}{\sqrt{3/2f_{a_1}^2 + f_{\pi_h}^2}}. \quad (64)$$

Then, when we substitute  $a$  into Eq. (62), the decay constant of the axion is

$$F_a = \frac{2\sqrt{3/2f_{a_1}^2 + f_{\pi_h}^2}}{\sqrt{6}}. \quad (65)$$

The  $g_{a\gamma\gamma}^{\text{UV}}$  of  $a$  coming from  $\pi_h^{15}$  to  $\gamma\gamma$  is given as<sup>3</sup>

$$\mathcal{L}_{\pi_h^{15}\gamma\gamma} = \frac{3\sqrt{6}}{2}(q_\psi^2 - q_{Q'}^2) \frac{\pi_h^{15}}{f_{\pi_h}} \frac{\alpha_{\text{em}}}{4\pi} F^{\mu\nu} \tilde{F}_{\mu\nu}, \quad (66)$$

where  $q_\psi$  and  $q_{Q'}$  are the electric charges of the fermions  $\psi$  and  $Q'$ . Therefore, the UV contribution of the light axion is

<sup>3</sup>The  $a_1 F\tilde{F}$  term does not appear, since we do not rotate  $a_1$  into the fourth term in Eq. (62).

$$g_{a\gamma\gamma}^{\text{UV}} = 6(q_\psi^2 - q_{Q'}^2) \frac{\alpha_{\text{em}}}{2\pi F_a}. \quad (67)$$

In this model, the axion-photon coupling  $g_{a\gamma\gamma}^{\text{UV}}$  is contributed by the electric charge of fermions  $\psi$  and  $Q'$ . Furthermore, there are other colorless scalars:  $\pi_h^{15}$  with  $m_{\pi_h^{15}}^2 \sim f_{a_1}f_{\pi_h}$  and  $\rho$  with  $m_\rho^2 \sim f_{a_1}^2$ .

## V. CONCLUSION AND DISCUSSION

We investigate all possible solutions to the strong  $CP$  problem with anomalous  $U(1)$  global symmetries when the hidden QCD is introduced, which include both the Peccei-Quinn mechanism and dynamical solutions. We find that these two mechanisms can exist together, and a new class of solutions for the strong  $CP$  problem are proposed. Thus, we classify two  $U(1)$  models in a unified way and discuss both one- $U(1)$  and two- $U(1)$  solutions in this work.

A mooselike diagram method is used to illustrate how the strong  $CP$  problem is solved via cancellation between  $CP$  phases, which could be read directly. When the gauge interaction and new particles are given, a diagram can be determined with a breaking mode of  $U(1)$  symmetries. From these diagrams, cancellation between  $CP$  phases can

be easily read without a detailed analysis of the model. This information is important for solving the strong  $CP$  problem. This method could be used to find new types of solutions and easily extended to cases of multi- $U(1)$  and multigauge interactions.

In one-axion solutions, additional  $Z_2$  symmetry keeps  $\theta = \theta'$  for solving the strong  $CP$  problem. In two-axion solutions, two chiral  $U(1)$ 's [either  $U(1)_{PQ}$  or  $U(1)_A$ ] have to be introduced. As a consequence, there is always an invisible light axion and a heavy axion.

Using the diagram method, we find two new mixed solutions. In model A, the spontaneous breaking of  $U(1)_{PQ}$  symmetry is triggered by the scalar potential, independently of the confinement of the hidden QCD, and the axion-photon couplings  $g_{a\gamma\gamma}^{\text{UV}}$  and the light axion decay constant  $F_a$  are both inversely proportional to the difference of anomalous charges  $|m - n|$ . In model B,  $U(1)_{PQ}$  is induced by the confinement of the hidden QCD,  $g_{a\gamma\gamma}^{\text{UV}}$  is contributed by the electric charge of fermions  $\psi$  and  $Q'$ , which is unlike normal two-axion models. At low energy scales, it is hard to distinguish this light axion from the QCD axion, even when one extends the scenario to multi- $U(1)$  symmetries and multigauge interactions. However, this kind of solution could be probed by detecting particles at the hidden QCD scale. Those heavy particles may leave some hints in cosmology and at the colliders.

## ACKNOWLEDGMENTS

We would like to thank Qing-Hong Cao and Shou-hua Zhu for valuable discussions and their support. D. H. is supported in part by the National Science Foundation of China under Grants No. 11635001 and No. 11875072. H.-R. J. is supported in part by the National Science Foundation of China under Grants No. 11725520, No. 11675002, and No. 11635001. H.-L. L. and J.-H. Y. are supported by the National Science Foundation of China (NSFC) under Grant No. 11875003. M.-L. X. is supported by the NSFC under Grant No. 2019M650856 and the 2019 International Postdoctoral Exchange Fellowship Program. J.-H. Y. is also supported by the NSFC under Grant No. 11947302.

## APPENDIX A: DERIVING THE AXION MASS FROM THE POTENTIAL

The typical potentials involving axion and QCD mesons (or hidden QCD mesons if changing the relevant parameters to their counterparts) are prevalent in our paper. We show in the following that the presence of the  $\eta$  field simply leads to an effective potential that only involves the mixing between the light axion and the pion after integrating out the heavy  $\eta$  particle. The mass potential for the conventional QCD axion model reads

$$V = -2Af_\pi^3 \left[ m_u \cos\left(\frac{\pi^0 + \eta}{f_\pi}\right) + m_d \cos\left(\frac{\pi^0 - \eta}{f_\pi}\right) \right] + Bf_\pi^4 \left( \frac{2\eta}{f_\pi} + \theta + \frac{a}{f_a} \right)^2. \quad (\text{A1})$$

The second term coming from the instanton effect is usually much larger than the first term coming from chiral perturbation theory. Therefore, one can diagonalize the mass matrix among the  $\eta$  and  $a$  first, yielding a massive field  $\tilde{\eta}$  and a massless one  $\tilde{a}$  as mixings of the original  $\eta$  and  $a$ :

$$\begin{pmatrix} \tilde{a} \\ \tilde{\eta} \end{pmatrix} = \begin{pmatrix} \cos \alpha & -\sin \alpha \\ \sin \alpha & \cos \alpha \end{pmatrix} \begin{pmatrix} a \\ \eta \end{pmatrix}, \quad (\text{A2})$$

where  $\sin \alpha$  and  $\cos \alpha$  are given by

$$\cos \alpha = \frac{2f_a}{\sqrt{f_\pi^2 + 4f_a^2}}, \quad \sin \alpha = \frac{f_\pi}{\sqrt{f_\pi^2 + 4f_a^2}}. \quad (\text{A3})$$

For  $f_a \gg f_\pi$ , we have  $\cos \alpha \sim 1$  and  $\sin \alpha \sim f_\pi/2f_a$ . Replacing  $\eta$  with  $\tilde{a}$  and  $\tilde{\eta}$  to the first term in  $V$ , we obtain

$$\begin{aligned} V_{\text{eff}} &= -2Af_\pi^3 \left[ m_u \cos\left(\frac{\pi^0 - \sin \alpha \tilde{a} + \cos \alpha \tilde{\eta}}{f_\pi}\right) + m_d \cos\left(\frac{\pi^0 + \sin \alpha \tilde{a} - \cos \alpha \tilde{\eta}}{f_\pi}\right) \right] \\ &\approx -2Af_\pi^3 \left[ m_u \cos\left(\frac{\pi^0}{f_\pi} - \frac{a}{2f_a}\right) + m_d \cos\left(\frac{\pi^0}{f_\pi} + \frac{a}{2f_a}\right) \right], \end{aligned} \quad (\text{A4})$$

where we use the approximation  $\tilde{a} \sim a$  and omit  $\tilde{\eta}$ , as it is a heavy particle. Now the remaining field  $\pi^0$  and  $a$  in the above potential can be further diagonalized to obtain the mass for  $a$  and  $\pi^0$ :

$$m_a = \frac{m_\pi f_\pi}{f_a} \frac{\sqrt{m_u m_d}}{(m_u + m_d)}, \quad (\text{A5})$$

$$m_{\pi^0} = \sqrt{2Af_\pi(m_u + m_d)}. \quad (\text{A6})$$

From Eqs. (A1)–(A3), one can see that the function of the field  $\eta$  is simply to move the axion fields into the cosine function with corresponding scale factor  $F_a$ .

### APPENDIX B: DYNAMICAL SYMMETRY BREAKING IN THE HIDDEN SECTOR

This Appendix shows the details of dynamical symmetry breaking in the hidden sector. The two specific examples in Figs. 1(b) and 2(b) are discussed. The  $su(N)$ -algebra is also shown in this Appendix.

In dynamical solutions, the global symmetries in the hidden sector are broken as

$$SU(N)_L \times SU(N)_R \times U(1)_A \times U(1)_V \rightarrow SU(N)_V \times U(1)_V, \quad (\text{B1})$$

$$T_1 = \begin{pmatrix} 0 & 1 & 0 & 0 \\ 1 & 0 & 0 & \vdots \\ 0 & 0 & 0 & 0 \\ \dots & & \ddots & \vdots \\ 0 & 0 & 0 & \dots & 0 \end{pmatrix}, \quad T_2 = \begin{pmatrix} 0 & -i & 0 & 0 \\ i & 0 & 0 & \vdots \\ 0 & 0 & 0 & 0 \\ \dots & & \ddots & \vdots \\ 0 & 0 & 0 & \dots & 0 \end{pmatrix}, \quad T_3 = \begin{pmatrix} 1 & 0 & 0 & 0 \\ 0 & -1 & 0 & \vdots \\ 0 & 0 & 0 & 0 \\ \dots & & \ddots & \vdots \\ 0 & 0 & 0 & \dots & 0 \end{pmatrix},$$

$$T_4 = \begin{pmatrix} 0 & 0 & 1 & 0 \\ 0 & 0 & 0 & \vdots \\ 1 & 0 & 0 & 0 \\ \dots & & \ddots & \vdots \\ 0 & 0 & 0 & \dots & 0 \end{pmatrix}, \quad \dots, \quad T_{N^2-1} = \sqrt{\frac{2}{N(N-1)}} \begin{pmatrix} 1 & 0 & 0 & 0 \\ 0 & 1 & 0 & \vdots \\ 0 & 0 & 1 & 0 \\ \dots & & \ddots & \vdots \\ 0 & 0 & 0 & \dots & 1-N \end{pmatrix}. \quad (\text{B4})$$

In general, scalars corresponding to diagonal generators and the identity matrix ought to be mixed.  $\eta'_h$  could be treated as an axion when instanton effects are the only source that explicitly breaks  $U(1)_A$ . Therefore, scalars corresponding to diagonal generators and identity matrix are important for solving the strong  $CP$  problem. The specific forms of diagonal generators and the identity matrix are

$$T_3 = \text{diag}(1, -1, 0, 0, \dots),$$

$$T_8 = \frac{1}{\sqrt{3}} \text{diag}(1, 1, -2, 0, \dots),$$

$$T_{15} = \frac{1}{\sqrt{6}} \text{diag}(1, 1, 1, -3, \dots),$$

$$T_{N^2-1} = \sqrt{\frac{2}{N(N-1)}} \text{diag}(1, 1, 1, \dots, 1-N),$$

$$I = \frac{1}{\sqrt{N}} \text{diag}(1, 1, 1, \dots, 1). \quad (\text{B5})$$

where  $U(1)_A$  is explicitly broken by instanton effects. The effective theory at low energy is assumed to be

$$\mathcal{L} = \frac{f_{\pi_h}^2}{4} \text{Tr}(\partial_\mu U \partial^\mu U^\dagger) + B' f_{\pi_h}^4 \left( \theta' + \frac{i}{2} \text{Tr}(\log U - \log U^\dagger) \right)^2, \quad (\text{B2})$$

with

$$U = \exp \left[ \frac{i(\pi_h^a T^a + I \eta'_h)}{f_{\pi_h}} \right], \quad (\text{B3})$$

where  $\pi_h^a$  are Goldstones corresponding to the  $SU(N)_A$  symmetry and  $\eta'_h$  is a pseudo Goldstone corresponding to the  $U(1)_A$  symmetry.  $T^a$  are basis elements of the  $su(N)$  algebra and  $I$  is the  $N$ -dimensional identity matrix. We choose  $\text{tr}(T^a T^b) = 2\delta^{ab}$  as the normalization condition. Therefore,  $T^a$  are shown as

In the model shown in Fig. 1(b), vectorlike fermions  $\psi(3,3)$  and  $\chi(1,3)$  are introduced. In this case,  $\Psi = (\psi_1^C, \psi_2^C, \psi_3^C, \chi^C)$  has an  $SU(4)_L \times SU(4)_R$  flavor symmetry in the hidden sector under which  $\Psi$  transforms as

$$\Psi \rightarrow e^{i(\theta_a^L T^a P_L + \theta_a^R T^a P_R)} \Psi = e^{i(\theta_a^V T^a + \theta_a^A T^a \gamma^5)} \Psi. \quad (\text{B6})$$

For  $SU(4)$ , the diagonal generators are  $T_3$ ,  $T_8$ , and  $T_{15}$ . After the condensate of hidden QCD,  $\pi_h^a$  are Goldstones corresponding to coset generators of  $SU(4)_L \times SU(4)_R / SU(4)_V$ . The decomposition of  $\pi_h^a$  into  $SU(3)_c$  is

$$15 = 8 + 3 + \bar{3} + 1. \quad (\text{B7})$$

Colorless scalars are  $\pi_h^{15}$  and  $\eta'_h$ , corresponding to  $\gamma^5 \otimes T_{15}$  and  $\gamma^5 \otimes I$ , respectively. The remaining 14 colored scalars acquire masses from gluon loops in the same way that  $\pi^\pm$

acquire larger mass  $\pi^0$  from photon loops. The mass splitting between  $\pi^\pm$  and  $\pi^0$  is estimated by [45]

$$m_{\pi^\pm}^2 - m_{\pi^0}^2 \approx \frac{(3 \ln 2)}{2\pi} \alpha_{\text{em}} m_\rho^2. \quad (\text{B8})$$

Similarly, we can estimate these colored scalar masses as

$$m_{\pi_h} \approx \left( \frac{C_2[R] \alpha_s(\Lambda_h)}{\alpha_{\text{em}}} \right)^{1/2} \frac{m_{\rho_h}}{m_\rho} = \left( \frac{C_2[R] \alpha_s(\Lambda_h)}{\alpha_{\text{em}}} \right)^{1/2} \frac{\Lambda_h}{\Lambda_{\text{QCD}}}, \quad (\text{B9})$$

where  $R$  is the presentation of  $\pi_h$  in QCD and  $C_2$  is the Dynkin index. In the last step we assume that  $m_{\rho_h}/m_\rho = \Lambda_h/\Lambda_{\text{QCD}}$ . These colored scalars obtain heavy masses as long as the scale  $\Lambda_h$  is high enough, while color-singlet bosons  $\pi_h^{15}$  and  $\eta'_h$  get masses via instanton effects of QCD and hidden QCD.

The currents corresponding to  $\pi_h^{15}$  and  $\eta'_h$  and their divergences are

$$\begin{aligned} J_\mu(\pi_h^{15}) &= \bar{\Psi} \gamma_\mu \gamma_5 T^{15} \Psi, \\ J_\mu(\eta'_h) &= \bar{\Psi} \gamma_\mu \gamma_5 I_{4 \times 4} \Psi, \\ \partial_\mu J^\mu(\pi_h^{15}) &= \frac{3}{\sqrt{6}} \frac{g^2}{16\pi^2} G_a^{\mu\nu} \tilde{G}_{a\mu\nu}, \\ \partial_\mu J^\mu(\eta'_h) &= \frac{3}{\sqrt{2}} \frac{g^2}{16\pi^2} G_a^{\mu\nu} \tilde{G}_{a\mu\nu} + 2\sqrt{2} \frac{g^2}{16\pi^2} G_A^{\mu\nu} \tilde{G}'_{A\mu\nu}. \end{aligned} \quad (\text{B10})$$

Matching with these currents, we can get the potential (for simplicity, we focus on the anomaly terms) of these composite axions at low energy as

$$\begin{aligned} V &= b f_\pi^4 \left( \frac{3}{\sqrt{6}} \frac{\pi_h}{f_{\pi_h}} + \frac{3}{\sqrt{2}} \frac{\eta'_h}{f_{\pi_h}} + \theta \right)^2 \\ &\quad + b' f_{\pi_h}^4 \left( \frac{2\sqrt{2}\eta'_h}{f_{\pi_h}} + \theta' \right)^2. \end{aligned} \quad (\text{B11})$$

At the minimal point of the potential, cancellation equations of the  $CP$  phases are

$$\begin{aligned} \theta_{\text{phy}} &= \theta + \frac{\sqrt{6}}{2} \frac{\langle \pi_h \rangle}{f_h} + \frac{3\sqrt{2}}{2} \frac{\langle \eta'_h \rangle}{f_h} = 0, \\ \theta'_{\text{phy}} &= \theta' + 2\sqrt{2} \frac{\langle \eta'_h \rangle}{f_h} = 0. \end{aligned} \quad (\text{B12})$$

In the model shown in Fig. 2(b), the fermion  $\psi(3, 3)$  is introduced. In this case,  $N = 3$ ,  $\Psi = (\psi_1^C, \psi_2^C, \psi_3^C)$ . The only colorless scalar is  $\eta'_h$ , corresponding to  $I\gamma^5$ . The current and its divergence are

$$\begin{aligned} J_\mu(\eta'_h) &= \bar{\Psi} \gamma_\mu \gamma_5 I_{3 \times 3} \Psi, \\ \partial_\mu J^\mu(\eta'_h) &= \frac{\sqrt{6}g^2}{16\pi^2} G_a^{\mu\nu} \tilde{G}_{a\mu\nu} + \frac{\sqrt{6}g^2}{16\pi^2} G_A^{\mu\nu} \tilde{G}'_{A\mu\nu}. \end{aligned} \quad (\text{B13})$$

The corresponding potential of the composite axion at low energy is

$$V = b f_\pi^4 \left( \frac{\sqrt{6}\eta'_h}{f_{\pi_h}} + \theta \right)^2 + b' f_{\pi_h}^4 \left( \frac{\sqrt{6}\eta'_h}{f_{\pi_h}} + \theta' \right)^2. \quad (\text{B14})$$

At the minimal point of the potential, the cancellation equation of the  $CP$  phases is

$$\theta'_{\text{phy}} = \theta_{\text{phy}} = \theta + \sqrt{6} \frac{\langle \eta'_h \rangle}{f_{\pi_h}} = 0. \quad (\text{B15})$$

- 
- [1] G. 't Hooft, Symmetry Breaking through Bell-Jackiw Anomalies, *Phys. Rev. Lett.* **37**, 8 (1976).  
 [2] G. 't Hooft, Computation of the quantum effects due to a four-dimensional pseudoparticle, *Phys. Rev. D* **14**, 3432 (1976).  
 [3] C. A. Baker, D. D. Doyle, P. Geltenbort, K. Green, M. G. D. van der Grinten, P. G. Harris, P. Iaydjiev, S. N. Ivanov, D. J. R. May, J. M. Pendlebury, J. D. Richardson, D. Shiers, and K. F. Smith, Improved Experimental Limit on the Electric Dipole Moment of the Neutron, *Phys. Rev. Lett.* **97**, 131801 (2006).  
 [4] A. Nelson, Naturally weak  $CP$  violation, *Phys. Lett.* **136B**, 387 (1984).  
 [5] S. M. Barr, Solving the Strong  $CP$  Problem without the Peccei-Quinn Symmetry, *Phys. Rev. Lett.* **53**, 329 (1984).  
 [6] J. Gasser and H. Leutwyler, Quark masses, *Phys. Rep.* **87**, 77 (1982).  
 [7] R. D. Peccei and H. R. Quinn,  $CP$  Conservation in the Presence of Pseudoparticles, *Phys. Rev. Lett.* **38**, 1440 (1977).  
 [8] R. D. Peccei and H. R. Quinn, Constraints imposed by  $CP$  conservation in the presence of pseudoparticles, *Phys. Rev. D* **16**, 1791 (1977).  
 [9] S. Weinberg, A New Light Boson?, *Phys. Rev. Lett.* **40**, 223 (1978).  
 [10] F. Wilczek, Problem of Strong  $P$  and  $T$  Invariance in the Presence of Instantons, *Phys. Rev. Lett.* **40**, 279 (1978).  
 [11] W. A. Bardeen, R. Peccei, and T. Yanagida, Constraints on variant axion models, *Nucl. Phys.* **B279**, 401 (1987).  
 [12] J. E. Kim, Weak-Interaction Singlet and Strong  $CP$  Invariance, *Phys. Rev. Lett.* **43**, 103 (1979).

- [13] M. Shifman, A. Vainshtein, and V. Zakharov, Can confinement ensure natural  $CP$  invariance of strong interactions?, *Nucl. Phys.* **B166**, 493 (1980).
- [14] M. Dine, W. Fischler, and M. Srednicki, A simple solution to the strong  $CP$  problem with a harmless axion, *Phys. Lett.* **104B**, 199 (1981).
- [15] A. Zhitnitskii, Possible suppression of axion-hadron interactions, *Sov. J. Nucl. Phys. (Engl. Transl.)* **31**, 260 (1980).
- [16] G. G. Raffelt, Astrophysical axion bounds, in *Axions: Theory, Cosmology, and Experimental Searches*, Lecture Notes in Physics, Vol. 741, edited by M. Kuster, G. Raffelt, and B. Beltrán (Springer, Berlin, 2008), pp. 51–71.
- [17] S. M. Barr and D. Seckel, Planck-scale corrections to axion models, *Phys. Rev. D* **46**, 539 (1992).
- [18] M. Kamionkowski and J. March-Russell, Planck-scale physics and the Peccei-Quinn mechanism, *Phys. Lett. B* **282**, 137 (1992).
- [19] A. Hook, Tasi lectures on the strong  $CP$  problem and axions, *Proc. Sci.*, TASI2018 (2019) 004 [arXiv:1812.02669].
- [20] J. E. Kim, H. P. Nilles, and M. Peloso, Completing natural inflation, *J. Cosmol. Astropart. Phys.* **01** (2005) 005.
- [21] K. Choi, H. Kim, and S. Yun, Natural inflation with multiple sub-Planckian axions, *Phys. Rev. D* **90**, 023545 (2014).
- [22] T. Higaki, K. S. Jeong, N. Kitajima, and F. Takahashi, Quality of the Peccei-Quinn symmetry in the aligned QCD axion and cosmological implications, *J. High Energy Phys.* **06** (2016) 150.
- [23] Q. Bonnefoy, E. Dudas, and S. Pokorski, Axions in a highly protected gauge symmetry model, *Eur. Phys. J. C* **79**, 31 (2019).
- [24] H. Fukuda, K. Harigaya, M. Ibe, and T. T. Yanagida, A model of visible QCD axion, *Phys. Rev. D* **92**, 015021 (2015).
- [25] L. Randall, Composite axion models and Planck scale physics, *Phys. Lett. B* **284**, 77 (1992).
- [26] M. J. Strassler and K. M. Zurek, Echoes of a hidden valley at hadron colliders, *Phys. Lett. B* **651**, 374 (2007).
- [27] C. Kilic, T. Okui, and R. Sundrum, Vectorlike confinement at the LHC, *J. High Energy Phys.* **02** (2010) 018.
- [28] Z. Chacko, H.-S. Goh, and R. Harnik, Natural Electroweak Breaking from a Mirror Symmetry, *Phys. Rev. Lett.* **96**, 231802 (2006).
- [29] S. Weinberg, Larger Higgs-Boson-Exchange Terms in the Neutron Electric Dipole Moment, *Phys. Rev. Lett.* **63**, 2333 (1989).
- [30] M. Pospelov and A. Ritz, Electric dipole moments as probes of new physics, *Ann. Phys. (Amsterdam)* **318**, 119 (2005).
- [31] V. A. Rubakov, Grand unification and heavy axion, *J. Exp. Theor. Phys.* **65**, 621 (1997).
- [32] Z. Berezhiani, L. Gianfagna, and M. Giannotti, Strong  $CP$  problem and mirror world: The Weinberg-Wilczek axion revisited, *Phys. Lett. B* **500**, 286 (2001).
- [33] A. Albaid, M. Dine, and P. Draper, Strong  $CP$  and  $SU(2)_2$ , *J. High Energy Phys.* **12** (2015) 046.
- [34] A. Hook, Anomalous Solutions to the Strong  $CP$  Problem, *Phys. Rev. Lett.* **114**, 141801 (2015).
- [35] C.-W. Chiang, H. Fukuda, M. Ibe, and T. T. Yanagida, 750 GeV diphoton resonance in a visible heavy QCD axion model, *Phys. Rev. D* **93**, 095016 (2016).
- [36] K. Choi and J. E. Kim, Dynamical axion, *Phys. Rev. D* **32**, 1828 (1985).
- [37] T. Gherghetta, N. Nagata, and M. Shifman, A visible QCD axion from an enlarged color group, *Phys. Rev. D* **93**, 115010 (2016).
- [38] P. Agrawal, J. Fan, M. Reece, and L.-T. Wang, Experimental targets for photon couplings of the QCD axion, *J. High Energy Phys.* **02** (2018) 006.
- [39] P. Sikivie, Axions, Domain Walls, and the Early Universe, *Phys. Rev. Lett.* **48**, 1156 (1982).
- [40] R. Kappl, S. Krippendorf, and H. P. Nilles, Aligned natural inflation: Monodromies of two axions, *Phys. Lett. B* **737**, 124 (2014).
- [41] *Axions: Theory, Cosmology, and Experimental Searches*, Lecture Notes in Physics, Vol. 741, edited by M. Kuster, G. Raffelt, and B. Beltrán (Springer, Berlin, 2008).
- [42] G. G. di Cortona, E. Hardy, J. P. Vega, and G. Villadoro, The QCD axion, precisely, *J. High Energy Phys.* **01** (2016) 034.
- [43] L. D. Luzio, M. Giannotti, E. Nardi, and L. Visinelli, The landscape of QCD axion models, *Phys. Rep.* **870**, 1 (2020).
- [44] D. E. Kaplan and R. Rattazzi, Large field excursions and approximate discrete symmetries from a clockwork axion, *Phys. Rev. D* **93**, 085007 (2016).
- [45] T. Das, G. S. Guralnik, V. S. Mathur, F. E. Low, and J. E. Young, Electromagnetic Mass Difference of Pions, *Phys. Rev. Lett.* **18**, 759 (1967).